GHGs are largely removed from the atmosphere by the time ΔT reaches values where the 'hockey-stick' damage function is sharply nonlinear. For the longer-lived GHGs, the resulting EDI is modestly smaller than the EDI with $\gamma = 3$.

The timing of GHG emissions is of central interest for policy[11,25]. The EDI can be used to compare incremental emissions at different dates, for example 2005 and 2015, using CO_2 emissions in 1995 as the base. The EDI for CO_2 increases then decreases with decadal CO_2 emission delays, reflecting the opposing effects of increasing the incremental forcing in future years when incremental damages are larger but discounting is greater. EDIs for CH_4 decrease with emission year as emissions are delayed; those for the other GHGs considered increase with emission year. These results suggest that the welfare loss from climate change associated with IS92a emissions could be reduced by incrementally reallocating CO_2 emissions from 2005 to 1995 and 2015, delaying CH_4 emissions from 1995, and advancing emissions of N_2O, CFC-11, CFC-12 and HCFC-22 from 2005 and 2015 to 1995.

As the effects of climate change may depend more on its rate than its magnitude, damage functions based on $d[\Delta T(t)]/dt$ have been proposed[26]. Application of such functions to EDI is problematical, because the effect of an incremental emission is to first increase then decrease $d[\Delta T(t)]/dt$ as a function of t; for typical parameter values, the integrated incremental damages are negative. Viewing EDI as a function of the integration horizon, it starts positive, turns negative if either numerator or denominator changes sign before the other, then turns positive when both terms become less than zero (with a singularity when the denominator equals zero). For long integration horizons, EDIs calculated using a damage function equal to $\{d[\Delta T(t)]/dt\}^{\gamma}$ typically approximate the corresponding EDIs using D_{γ}.

Neither the GWP nor the EDI as defined here incorporate the effect of uncertainties on policy choice. Because information about climate change, its consequences, and mitigation approaches will change over time, near-term policies should be designed to accommodate sequential change[11]. With uncertainty, emissions of long-lived GHGs like CO_2 are more costly than emissions of shorter-lived GHGs like CH_4, because they constrain the set of achievable future climate states more severely. It may be useful to characterize uncertainty about $\Delta T_{2\times}$ and other parameters using probability distributions, and to incorporate the economic value of the option to decrease future radiative forcing that is lost by emitting longer-lived GHGs in an extended EDI.

Values of EDI are broadly comparable in magnitude and in range of uncertainty to GWP. Nevertheless, EDI offers significant advantages for policy analysis. Because EDI is defined in terms of economic welfare, it is directly relevant to policy choice; moreover, questions about the damage function and discount rate are clearly defined and may be addressed by research on climate impacts and preferences for impacts at different dates. EDI can also incorporate non-climate effects of GHG emissions on welfare, such as CO_2 fertilization and stratospheric-ozone depletion. In contrast, GWP does not measure welfare changes, non-climate effects cannot be incorporated, and the appropriate time horizon cannot be determined by analysis[4–7]. Uncertainty about the appropriate values of EDI may be an accurate reflection of uncertainty about the consequences for welfare of climate change, rather than a limitation of the index. □

Received 13 October 1995; accepted 17 April 1996.

1. Shine, K. P., Derwent, R. G., Wuebbles, D. J. & Morcrette, J.-J. in *Climate Change: The IPCC Scientific Assessment* (eds Houghton, J. T., Jenkins, G. J. & Ephraums, J. J.) 41–68 (Cambridge Univ. Press, 1990).
2. Isaksen, I. S. A., Ramaswamy, V., Rodhe, H. & Wigley, T. M. L. in *Climate Change 1992: The Supplementary Report to the IPCC Scientific Assessment* (eds Houghton, J. T., Callander, B. A. & Varney, S. K.) 47–67 (Cambridge Univ. Press, 1992).
3. Albritton, D. L., Derwent, R. G., Isaksen, I. S. A., Lal, M. & Wuebbles, D. J. in *Climate Change 1994: Radiative Forcing of Climate Change and an Evaluation of the IPCC IS92 Emissions Scenarios* (eds Houghton, J. T. et al.) 205–231 (Cambridge Univ. Press, 1995).
4. Eckaus, R. S. *Energy J.* **13,** 25–35 (1992).
5. Reilly, J. M. & Richards, K. R. *Envir. Resourc. Econ.* **3,** 41–61 (1993).
6. Schmalensee, R. *Energy J.* **14,** 245–255 (1993).
7. Kandlikar, M. *Energy Policy* **23,** 879–883 (1995).
8. Cropper, M. L. & Oates, W. E. *J. econ. Literat.* **30,** 675–740 (1992).
9. Victor, D. G. *Policy Sci.* **24,** 199–222 (1991).
10. Lashof, D. A. & Ahuja, D. R. *Nature* **344,** 529–531 (1990).
11. Hammitt, J. K., Lempert, R. J. & Schlesinger, M. E. *Nature* **357,** 315–318 (1992).
12. Wuebbles, D. J., Jain, A. K., Patten, K. O. & Grant, K. E. *Clim. Change* **29,** 265–297 (1995).
13. Nordhaus, W. D. *Science* **258,** 1315–1319 (1992).
14. Peck, S. C. & Teisberg, T. J. *Energy J.* **13,** 55–77 (1992).
15. Manne, A., Mendelsohn, R. & Richels, R. *Energy Policy* **23,** 17–34 (1995).
16. Leggett, J., Pepper, W. & Swart, R. in *Climate Change 1992: The Supplementary Report to the IPCC Scientific Assessment* (eds Houghton, J. T., Callander, B. A. & Varney, S. K.) 69–95 (Cambridge Univ. Press, 1992).
17. Mitchell, J. F. B., Manabe, S., Meleshko, V. & Tokioka, T. in *Climate Change: The IPCC Scientific Assessment* (eds Houghton, J. T., Jenkins, G. J. & Ephaums, J. J.) 131–172 (Cambridge Univ. Press, 1990).
18. Gates, W. L., Mitchell, J. F. B., Boer, G. J., Cubash, U. & Meleshko, V. P. in *Climate Change 1992: The Supplementary Report to the IPCC Scientific Assessment* (eds Houghton, J. T., Callander, B. A. & Varney, S. K.) 97–134 (Cambridge Univ. Press, 1992).
19. Jain, A. K., Kheshgi, H. S. & Wuebbles, D. J. *Integrated Science Model for Assessment of Climate Change* (UCRL-JC 116526; Lawrence Livermore National Lab., Livermore, CA, 1994).
20. Jain, A. K., Kheshgi, H. S., Hoffert, M. I. & Wuebbles, D. J. *Global biogeochem. Cycles* **9,** 153–166 (1995).
21. Schimel, D. S. *et al.* in *Climate Change 1994: Radiative Forcing of Climate Change and an Evaluation of the IPCC IS92 Emissions Scenarios* (eds Houghton, J. T. *et al.*) 35–71 (Cambridge Univ. Press, 1995).
22. Enting, I. G., Wigley, T. M. L. & Heimann, M. *Future Emissions and Concentrations of Carbon Dioxide: Key Ocean/Atmosphere/Land Analyses* (Division of Atmospheric Res., CSIRO, Australia, 1995).
23. Bacastow, R. & Keeling, C. D. in *Carbon in the Biosphere* (eds Woodwell, G. M. & Pecan, E. V.) 86–135 (NTIS, Springfield, Virginia, 1973).
24. Bretherton, F. P., Bryan, K. & Woods, J. D. in *Climate Change: The IPCC Scientific Assessment* (eds Houghton, J. T., Jenkins, G. J. & Ephaums, J. J.) 173–193 (Cambridge Univ. Press, 1990).
25. Schlesinger, M. E. & Jiang, X. *Nature* **350,** 219–221 (1991).
26. Peck, S. C. & Teisberg, T. J. *Clim. Change* **28,** 289–315 (1994).

ACKNOWLEDGEMENTS. This work was supported by the US Department of Energy, Office of Health and Environmental Research.

Occurrence patterns of foreshocks to large earthquakes in the western United States

Rachel E. Abercrombie*† & Jim Mori‡

* Department of Earth Sciences, University of Southern California, Los Angeles, California, 90089, USA
‡ US Geological Survey, Pasadena, California, USA

Observations of foreshocks preceding large earthquakes provide one of the few well documented cases of premonitory events that are clearly related to a subsequent earthquake. Unfortunately, the apparent randomness of foreshock occurrence—they precede some events and not others—has severely hampered their use in reliable earthquake prediction. Understanding the factors that control foreshock occurrence is critical for determining how large earthquakes initiate and whether reliable short-term prediction will ever be possible[1]. Here we report the results of a comprehensive study of the occurrence patterns of foreshocks to large earthquakes in the western United States. The incidence of foreshocks decreases with increasing depth of the mainshock, and also depends on the mainshock slip orientation. This pattern of occurrence may be explained by a decrease in small-scale crustal heterogeneity with increasing depth, and suggests that increasing normal stress (both regional tectonic stress and lithostatic load) inhibits the occurrence of foreshocks. No relationship is observed between any aspect of foreshock occurrence and the magnitude of the subsequent mainshock, suggesting that

† Present address: Institute of Geological and Nuclear Sciences, Kelburn Research Centre, 32 Salamanca Road, PO Box 1320, Wellington, New Zealand.

the eventual size of the mainshock may be independent of the earthquake nucleation process, or that foreshocks are not part of this process.

Earthquakes are sometimes preceded by single or multiple events of smaller magnitude, known as foreshocks[2]. How foreshocks are related to the subsequent large earthquake (mainshock) and why they precede some and not others is still unknown. Most theories assume that heterogeneity in the crust contributes to foreshock occurrence[2]. For example, foreshock occurrence has been related to heterogeneities within a zone of accelerating preseismic slip, similar to that observed in laboratory experiments[3,4]. Previous studies of foreshocks have been limited by the data quantity and quality. Attempts to find any relationship between characteristics of the foreshock sequences and the mainshock magnitude have been unsuccessful[5–7]. In California, a possible decrease in foreshock sequence duration with mainshock depth was noted[5], as was a greater tendency for more strike-slip earthquakes to have foreshocks than thrusts, but the available data were insufficient to produce a convincing result. In the decade and more since these studies were performed, many earthquakes have been well recorded by the dense seismic networks operating in California and Nevada. Also, more seismometers and enhanced analysis techniques have lead to considerable improvement in resolution of source parameters such as earthquake depth and focal mechanism. This increase in both quantity and quality of available earthquake data now enables us to determine robust relationships governing foreshock occurrence. Here we focus on how foreshock occurrence is related to the hypocentral depth, style of faulting and magnitude of the subsequent mainshock in order to improve our understanding of the earthquake nucleation process.

The characteristics of foreshock occurrence can only be studied reliably in areas and time periods in which regional seismic networks are able to detect small earthquakes and in which many large earthquakes have occurred. The study areas selected are the parts of California and Nevada in which seismic networks have had complete detection of earthquakes with magnitude $M \geqslant 2$ since 1975. Excluding aftershocks and swarm activity immediately around the Mammoth Lakes volcanic area, 59 earthquakes with $M \geqslant 5$ occurred during this period (Table 1, Fig. 1). The network catalogues were searched for immediate foreshocks, $M \geqslant 2$, occurring within 5 km and 30 days of these large earthquakes. Such small limits in time and space were chosen as these events can most clearly be related to the nucleation of the subsequent large earthquake[8]. Also, tight spatial and temporal limits enable foreshocks to be distinguished easily from background seismicity. In all but one sequence, foreshocks continued to within 24 hours of the mainshock.

There is no clear geographical separation of earthquakes with and without foreshocks, although a slightly higher proportion of earthquakes in the Mojave shear zone and along the California–Nevada border have foreshocks than along the San Andreas fault zone. We therefore analyse the data set as a whole and find that 44% of the earthquakes in the whole data set had foreshocks,

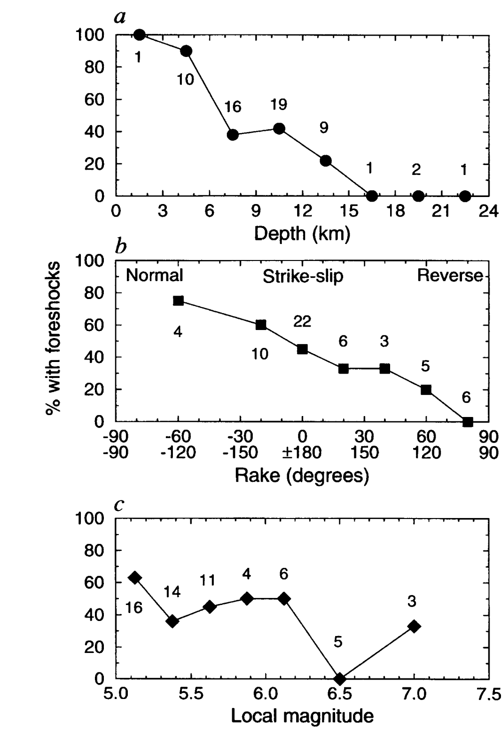

FIG. 2 Foreshock occurrence as a function of mainshock (*a*) depth, (*b*) rake, and (*c*) magnitude. A rake of $-90°$ corresponds to normal faulting, 0° and $\pm180°$ correspond to strike-slip motion, and 90° to reverse or thrust faulting. The data are from Table 1 and the numbers above or below each data point correspond to the total number of mainshocks in that interval. The occurrence pattern of foreshocks is dependent on the depth and style of faulting of the mainshock, but appears independent of the mainshock magnitude. We investigated these relationships using the Student's *t*-test to evaluate the difference between populations[56]. The cumulative sum curve of $1-p$ (if the event has foreshocks) and $-p$ (no foreshocks) against depth was plotted, where p is the proportion of earthquakes in the whole data set with foreshocks. The earthquakes were then divided into three depth ranges at the two gradient changes in the cumulative sum: $\leqslant 8.3$ km, 8.3–12.1 km and >12.1 km (80%, 33% and 1% having foreshocks, respectively). We found the shallowest group to be different from the others at the 99% significance level, and the deeper groups significantly different from one another at the 95% confidence level. Similarly we divided the earthquakes into two populations with 'rake' $\leqslant 20°$ and $>20°$ (52% and 13% having foreshocks, respectively) and these were found to be different at the 99% confidence level. Dividing the data set by magnitude (for example, at magnitude 5.5 or 6) however, produced no statistically significant difference in the populations.

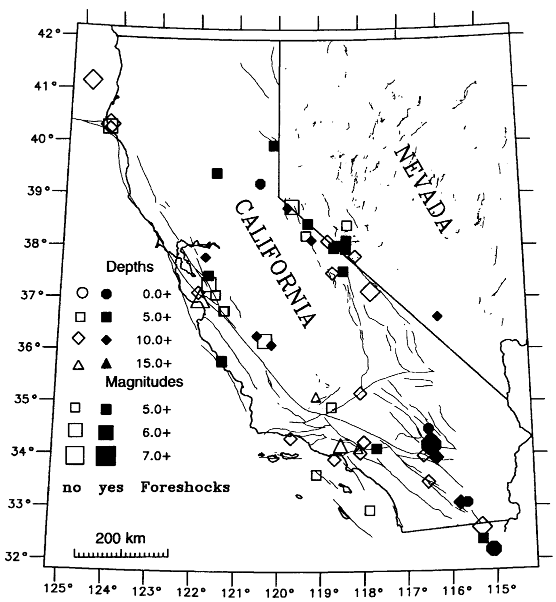

FIG. 1 Map showing the locations of the 59 $M \geqslant 5$ earthquakes included in this study. The symbols are depth-dependent; filled symbols indicate earthquakes preceded by immediate foreshocks, and open symbols, those without. In the case of multiple earthquake sequences, the first earthquake with $M \geqslant 5$ is considered the mainshock and later events are not included in this study, as the foreshocks of the later events cannot be distinguished from the aftershocks of the first.

TABLE 1 Hypocentral parameters of the $M \geqslant 5$ earthquakes considered in this study

Date (Yr/month/d h:min:s)		Name	Lat. (°)	Long. (°)	Depth (km)	M_L	Strike (°)	Dip (°)	Rake (°)	N	Duration (h)
1975/6/1	01:38:49	Galway Lake[21]	34.52	116.50	4.5*	5.0	160	70	180	6	720
1975/8/1	20:20:05	Oroville[22]	39.45	121.54	5.5	5.7	180	65	−70	11	720
1977/2/22	06:24:06	Bridgeport Is.[TS]	38.49	119.29	6.7*	5.0				1	116.98
1978/8/13	22:54:53	Santa Barbara[23]	34.35	119.70	12.8*	5.1	280	27	57	–	–
1978/9/4	21:54:52	Diamond Valley[24]	38.79	119.79	10.1*	5.2	315	80	160	9	34.483
1978/10/4	16:42:48	Wheeler Crest[25]	37.53	118.70	14.9	5.4	015	90	10	–	–
1979/1/1	23:14:39	New Year/Malibu[26]	33.94	118.68	11.3*	5.2	280	60	85	–	–
1979/2/22	15:57:29	Doyle[27]	39.99	120.12	8.2*	5.3	40	70	−20 (−160)	1	8.67
1979/3/15	21:07:16	Homestead Valley[28]	34.33	116.44	2.5*	5.3			180	19	720
1979/8/6	17:05:22	Coyote Lake[29]	37.10	121.51	8.9*	5.8	024	80	180	–	–
1979/10/7	20:54:40	Bridgeport II[30]	38.23	119.35	8.4*	5.0	150	90	165 (0)	–	–
1979/10/15	23:16:53	Imperial Valley[31]	32.61	115.32	12.3*	6.4	323	90	180	–	–
1980/1/24	19:00:08	Livermore Valley[32]	37.83	121.77	11.8	5.8	167	85	−160	1	0.0242
1980/2/25	10:47:38	Anza/White Wash[33]	33.50	116.51	12.7	5.5	305	70	−162	–	–
1980/6/9	03:28:19	Victoria[31]	32.19	115.08	4.6*	6.1	318	90	180	2	480
1980/6/29	07:46:13		38.01	118.66	9.3*	5.0				1	0.0242
1980/9/7	01:30:42	ref. 30	38.07	118.58	8.3*	5.1	74	72	0 (162)	21	43.412
1980/11/8	10:27:30	Eureka[34]	41.15	124.75	11.0	6.9	45	90	0	–	–
1980/11/28	18:21:13	ref. 35	39.26	120.46	3.6*	5.1	219	80	10 (170)	2	1.159
1980/12/28	22:58:08	ref. 30	38.16	118.37	6.9*	5.1	248	77	−20 (−15)	5	26.91
1981/4/26	12:09:28	Westmoreland[36]	33.10	115.63	3.8*	5.7	∼200	∼60	∼−50 (∼−140)	85	120
1981/9/4	15:50:50	Catalina[TS]	33.65	119.09	6.0*	5.5	325	90	−152	–	–
1982/9/24	07:40:24	ref. 30	37.85	118.16	10.7*	5.5	248	77	−20 (−166)	–	–
1982/10/25	22:26:03		36.32	120.51	12.1*	5.4				3	1.809
1982/12/28	19:06:24	ref. 30	37.99	118.39	9.1	5.2	162	61	−163 (−30)	2	5.217
1983/5/2	23:42:38	Coalinga[37]	36.23	120.32	9.8*	6.7	127	23	90	–	–
1983/8/29	10:10:31	San Simeon Is.[TS]	35.84	121.34	5.9*	5.2	311	51	133	3	21.74
1984/4/24	21:15:18	Morgan Hill[38]	37.31	121.68	8.6*	6.2	325	90	175	–	–
1985/1/24	11:27:21	ref. 30	38.15	118.82	13.3*	5.3	202	80	0 (−170)	–	–
1985/8/4	12:01:55	Kettleman Hills[39]	36.14	120.15	10.1	5.6	145	25	110	6	22.079
1986/1/26	19:20:50	TS	36.80	121.28	8.9*	5.5	350	90	165	–	–
1986/3/31	11:55:39	Mount Lewis[40]	37.48	121.68	8.1	5.7	355	80	175	3	178
1986/7/8	09:20:44	North Palm Springs[41]	34.00	116.61	11.4	5.6	300	45	180	–	–
1986/7/13	13:47:08	Oceanside[42]	32.97	117.87	8.8	5.4	110	50	70	–	–
1986/7/20	14:29:45	Chalfant[KS]	37.57	118.44	6.7*	5.9	220	65	−10	13	168
1987/2/7	03:45:14	North Cerro Prieto[TS]	32.39	115.31	6.0*	5.4			180	2	15.77
1987/10/1	14:42:20	Whittier[43]	34.06	118.09	14.6	5.9	270	25	90	–	–
1987/11/24	01:54:14	Elmore Ranch[44,45]	33.09	115.79	10.6	6.2	217	79	4	2	0.357
1988/2/20	08:39:57	TS	36.79	121.31	9.7*	5.1	135	50	10	–	–
1988/6/10	23:06:43	Gorman[TS]	34.94	118.74	6.8*	5.4	155	65	150	–	–
1988/9/19	02:56:31	Garfield Hills[30]	38.46	118.34	9.0	5.3	138	85	−175 (−5)	–	–
1988/12/3	11:38:26	Pasadena[46]	34.15	118.13	15.5	5.0	245	70	0	–	–
1989/8/8	08:13:27	Lake Elsman[TS]	37.14	121.93	13.9*	5.4	301	63	152	–	–
1989/10/18	00:04:15	Loma Prieta[47,48]	37.04	121.88	19.0	7.0	130	70	135	–	–
1990/2/28	23:43:36	Upland[49]	34.14	117.69	5.5	5.4	310	70	0	2	3.104
1990/10/24	06:15:19	Lee Vining[30,50]	38.05	119.12	11.7	5.6	55	60	−10	1	0.0022
1991/6/28	14:43:54	Sierra Madre[51]	34.26	118.00	12.0	5.4	242	50	90	–	–
1991/8/17	19:29:40	Honeydew[52]	40.29	124.24	8.5*	6.0	311	22	51	–	–
1991/9/17	21:10:29	San Simeon II[MP]	35.82	121.33	8.0	5.2	297	64	113	–	–
1992/3/8	03:43:04	Petrolia[52]	40.26	124.23	10.7*	5.3	120	90	180	–	–
1992/4/23	04:50:23	Joshua Tree[53]	33.96	116.32	14.4	6.1	340	90	160	5	2.415
1992/4/25	18:06:05	Petrolia[54]	40.33	124.23	10.6	6.5	350	13	106	–	–
1992/6/28	11:57:34	Landers[53]	34.20	116.44	4.5	7.3	350	90	170	19	720
1992/6/29	10:14:20	Little Skull Mtn[KS]	36.72	116.31	11.8	5.2	60	70	−70	3	9.760
1992/7/11	18:14:16	Mojave[TS]	35.21	118.07	10.7*	5.7	20	80	30	–	–
1993/5/17	23:20:49	Eureka Valley[KS]	37.17	117.79	11.9	6.1	174	32	−126	–	–
1993/5/28	04:47:40	Wheeler Ridge[TS]	35.15	119.10	21.4*	5.2			∼180	–	–
1994/1/17	12:30:55	Northridge[55]	34.21	118.54	18.7	6.7	105	35	100	–	–
1994/9/12	12:23:44	Double Spring Flat[KS]	38.83	119.66	8.0*	6.3	21	81	−25	–	–

N is the number of foreshocks with $M \geqslant 2$ occurring within 5 km horizontally and 30 days of the mainshock, and 'duration' is the duration of the foreshock sequence ($M \geqslant 2$). Earthquake names are included where assigned by previous authors. Focal mechanisms and hypocentral depths of the mainshocks are taken from detailed previous studies where available. First motion focal mechanisms are preferred as the most relevant to the nucleation process. An asterisk following the depth indicates that the catalogue depth is used. If the fault plane is unknown, the rake of the other plane is given in brackets. Focal mechanisms determined in this study are calculated as in ref. 37 using phase picks from the Californian catalogues. TS, this study; KS, K. Smith, personal communication; MP, M. Pasyanos, personal communication. The depths and focal mechanisms of the foreshocks are not considered as most are relatively poorly determined. The mean foreshock depths per sequence are highly correlated with the mainshock depths, however, (correlation coefficient, 0.63; significant at the 99% confidence level). Also, in detailed analyses of well recorded foreshock sequences, the depths and focal mechanisms of the foreshocks are very similar to those of the mainshock[15,40,44,49].

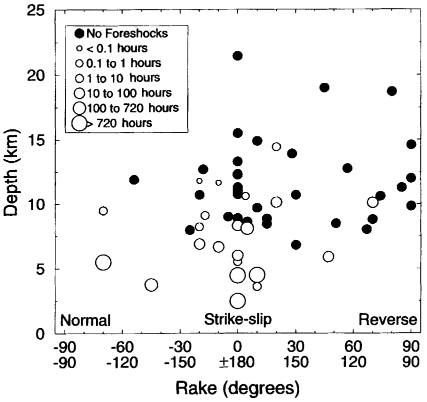

FIG. 3 Foreshock sequence occurrence and duration as a function of mainshock depth and slip orientation. The data are again taken from Table 1. In this dataset, the mean depth of reverse faulting earthquakes is slightly (but not significantly) greater than for normal faulting ones. Within the range −30° to 30° rake, where the depth range is constant, a decrease in foreshock occurrence with increasing rake is observed, so this relationship is not simply an artefact of the depth distribution.

similar to the number found in previous studies in the region[5,7,9]. It is worth noting, however, that foreshocks preceded only three earthquakes near the conurbations of Los Angeles and the Bay Area, suggesting that they may be of less use for urban hazard warnings in these areas than would be predicted from consideration of the whole data set.

Foreshock occurrence is plotted in Fig. 2 as a function of depth (Fig. 2*a*), slip orientation (Fig. 2*b*) and mainshock magnitude (Fig. 2*c*). Foreshock occurrence clearly decreases with increasing depth and is also dependent on the style of faulting. Most normal faulting earthquakes have foreshocks, compared to about half the strike-slip events and only very few of the reverse faulting ones. Both the relationships between foreshock occurrence and depth and rake are over 95% significant (Fig. 2). No relationship is observed, however, between the mainshock magnitude and the pattern of foreshock occurrence.

Normal stress increases both with depth and also from normal to reverse faulting environments[10], so it is plausible that foreshock occurrence is inhibited by increasing normal stress. Also, in Fig. 3, a tendency for the duration of foreshock sequences to decrease with increasing depth is seen; the correlation coefficient between the logarithm (base 10) of the duration of the foreshock sequence and mainshock depth is 0.61, 99% significant. This has previously been suggested from a smaller data set[5]. This observation supports the hypothesis that increasing normal stress (both regional tectonic stress and loading stress with depth) inhibits foreshock occurrence, and it seems that at high normal stress foreshock sequences tend to be short or non-existent.

Foreshocks, like other small earthquakes, can be interpreted as the breaking of small patches of fault as they reach a critical stress, but which do not propagate further to become large earthquakes. It would seem plausible, therefore, that more small earthquakes, and similarly more foreshocks, would occur in regions with a higher degree of small-scale heterogeneity. The idea of heterogeneity decreasing with depth and normal stress is not new, and is consistent with the frequency–magnitude statistics of earthquake occurrence in California; the ratio of small ($M = 2$) to larger earthquakes is greater at shallower depths than at deeper ones[11]. This result suggests that, in general, a dynamic rupture nucleating at depth is less likely to be stopped by small-scale heterogeneity—and more likely to grow into a larger earthquake—than a similar initiation at more shallow depths. This pattern is consistent with the observed depth-dependence of foreshock occurrence. Heterogeneity within fault zones affecting earthquake rupture could be compositional, or geometric, or related to spatial variations in fault gouge properties such as fluid pressures, or even aseismic creep. All of these are expected to vary with depth and normal stress, and discriminating amongst them will be difficult.

Laboratory studies of frictional sliding observe pre-seismic slip over a critical slip distance D_c before unstable dynamic failure[3,4]. D_c is observed to decrease in size with increasing stress and shear localization[12] and, therefore, may be expected to decrease with depth[13], and so be related to our foreshock observations. It is unclear, however, whether there is a direct connection, as D_c is estimated to have dimensions considerably smaller than the volumes in which foreshocks occur[14]. There is also no apparent reason why a change in D_c should inhibit foreshock occurrence. We therefore prefer the hypothesis of decreasing small-scale heterogeneity with depth, which also explains the observed depth dependence of the earthquake frequency–magnitude distribution.

Perhaps the most important question concerning earthquake nucleation is whether the magnitude of an earthquake is controlled primarily by its nucleation process (for example, the amount and area of pre-seismic slip), or whether all earthquakes initiate in a similar manner, and the final slip and rupture area depend on the local stress state[1] and on the dynamics of the earthquake rupture itself. The first, 'nucleation-controlled', scenario is the most optimistic for short-term prediction; the second, 'rupture-controlled' scenario implies that the magnitude of the earthquake is unknown until the rupture propagation stops. The role of foreshocks in the earthquake initiation process is still unclear. In the 'nucleation-controlled' model they could be interpreted as part of the nucleation process of a large event, probably caused by pre-seismic slip[4,15]. In the 'rupture-controlled' case, foreshocks are simply small earthquakes, easily stopped by the local heterogeneity, in the hypocentral region of the mainshock. The eventual mainshock is a rupture initiation which is not stopped and cascades into a larger earthquake. In this 'rupture-controlled' model, most small earthquakes will not evolve into large earthquakes, and foreshocks may not be different from other short sequences of smaller earthquakes which do not culminate in a larger event.[16]

Recent studies of the onset of large earthquakes[17,18] have found that they commonly initiate with a small subevent, <1% of the total seismic moment. These small initial subevents can also be interpreted in terms of the two models of earthquake initiation outlined above. In the 'rupture-controlled' model, they can be considered as ordinary small earthquakes (perhaps the last foreshocks?) which dynamically trigger a neighbouring large subevent[17]. Alternatively, in the 'nucleation-controlled' model, these initial subevents may be considered part of a nucleation phase with properties differing from a dynamic rupture, and whose size is related to that of the final earthquake[18].

No pre-seismic slip of the kind seen in laboratory experiments of frictional sliding has ever been unambiguously observed before earthquakes, however[19], indicating that if it does occur in the Earth, it must be very small. Some attempts to extrapolate the laboratory results to real crustal faults have proposed that pre-seismic slip could be related to the duration and volume of the foreshock sequence[4]. These models predict a correlation between the mainshock size and the spatial and temporal extent of the foreshock sequence, which can be investigated with the data collected in the present work. Other models, which do not imply size dependence[14,20], are more difficult to evaluate.

In the present study, no relationship is seen between the mainshock magnitude and foreshock occurrence (Fig. 2). We also find no relationship between mainshock magnitude and the logarithm (base 10) of the duration of the foreshock sequence (correlation coefficient, 0.17; 95% confidence limits −0.23 to 0.52), between the mainshock magnitude and the number of $M \geqslant 2$ foreshocks (correlation coefficient, 0.16; 95% confidence limits −0.24 to 0.51), or between mainshock magnitude and the magnitude of the largest foreshock (correlation coefficient, 0.17; 95% confidence limits −0.23 to 0.52). This is consistent with previous studies[5-7] which also found no relationship between foreshock occurrence and the magnitude of the subsequent mainshock. A relationship between the foreshock sequence and the subsequent mainshock magnitude is not explicitly required by the 'nucleation-controlled' model, although it has been suggested[4], and might be expected in a model in which the rupture is controlled by the nucleation process. The lack of a relationship between foreshock occurrence and mainshock magnitude observed here is therefore more consistent with the second ('rupture-controlled') model. □

Received 24 October 1995; accepted 16 April 1996.

1. Brune, J. N. *J. geophys. Res.* **84,** 2195–2198 (1979).
2. Mogi, K. *Bull. Earthquake Res. Inst.* **41,** 615–658 (1963).
3. Dieterich, J. H. *J. geophys. Res.* **84,** 2161–2168 (1979).
4. Ohnaka, M. *Tectonophysics* **211,** 149–178 (1992).
5. Jones, L. M. *Bull. seism. Soc. Am.* **74,** 1361–1380 (1984).
6. Jones, L. M. & Molnar, P. *J. geophys. Res.* **84,** 3596–3608 (1979).
7. Doser, D. I. *Bull. seism. Soc. Am.* **80,** 110–128 (1989).
8. Jones, L. M. *Bull. seism. Soc. Am.* **75,** 1669–1679 (1985).
9. Savage, M. K. & dePolo, D. M. *Bull. seism. Soc. Am.* **83,** 1910–1938 (1993).
10. Sibson, R. H. *Nature* **249,** 542–544 (1974).
11. Mori, J. & Abercrombie, R. E. *Eos (suppl.)* **76,** F388 (1995).
12. Marone, C. & Kilgore, B. *Nature* **362,** 618–621 (1993).
13. Scholz, C. H. *Nature* **336,** 761–763 (1988).
14. Dieterich, J. H. in *Earthquake Source Mechanics* (eds Das, S., Boatwright, J. & Scholz, C.) 37–47 (Am. Geophys. Un., Washington DC, 1986).
15. Dodge, D. A., Beroza, G. C. & Ellsworth, W. L. *J. geophys. Res.* **100,** 9865–9880 (1995).
16. Jones, L. M., Console, R., Di Luccio, F. & Murro, M. *Eos (suppl.)* **76,** F388 (1995).
17. Abercrombie, R. E. & Mori, J. *Bull. seism. Soc. Am.* **84,** 725–734 (1994).
18. Ellsworth, W. L. & Beroza, G. C. *Science* **268,** 851–855 (1995).
19. Wyatt, F. K., Agnew, D. C. & Gladwin, M. *Bull. seism. Soc. Am.* **84,** 768–779 (1994).
20. Dieterich, J. H. *Tectonophysics* **211,** 115–134 (1992).
21. Kanamori, H. & Fuis, G. *Bull. seism. Soc. Am.* **66,** 2017–2037 (1976).
22. Langston, C. A. & Butler, R. *Bull. seism. Soc. Am.* **66,** 1111–1120 (1976).
23. Corbett, E. J. & Johnson, C. E. *Bull. seism. Soc. Am.* **72,** 2201–2226 (1982).
24. Somerville, M. R., Peppin, W. A. & VanWormer, J. D. *Bull. seism. Soc. Am.* **70,** 1547–1555 (1980).
25. Peppin, W. A., Honjas, W., Sommerville, M. R. & Vetter, U. R. *Bull. seism. Soc. Am.* **79,** 67–76 (1989).
26. Hauksson, E. & Salvidar, G. V. *J. geophys. Res.* **94,** 9591–9606 (1989).
27. VanWormer, J. D. & Ryall, A. S. *Bull. seism. Soc. Am.* **70,** 1557–1572 (1980).
28. Hutton, L. K. *et al. Calif. Geol.* **33,** 110–114 (1980).
29. Liu, H.-L. & Helmberger, D. V. *Bull. seism. Soc. Am.* **73,** 201–218 (1983).
30. dePolo, C. M., Peppin, W. A. & Johnson, P. A. *Tectonophysics* **225,** 271–299 (1993).
31. Silva, P. & Masuda, T. *J. geophys. Res.* **90,** 7639–7651 (1985).
32. Bolt, B. A., McEvilly, T. V. & Urhammer, R. A. *Bull. seism. Soc. Am.* **71,** 451–463 (1981).
33. Given, J. W. thesis, California Inst. Technol. (1983).
34. Ekström, G. & Dziewonski, A. M. *Bull. seism. Soc. Am.* **75,** 23–39 (1985).
35. Vetter, U. R. & Ryall, A. S. *J. geophys. Res.* **88,** 8237–8250 (1983).
36. Frez, J. & Gonzalez, J. J. *The Gulf and Peninsular Provinces of the Californias* (Memoir 47, Am. Assoc. Petrol. Geol., Tulsa, Oklahoma, 1991).
37. Eaton, J. P. *Prof. Pap. U.S. geol. Surv.* **1487,** 113–170 (1990).
38. Oppenheimer, D. H., Reasenberg, P. A. & Simpson, R. W. *J. geophys. Res.* **93,** 9007–9026 (1988).
39. Ekström, G., Stein, R. S., Eaton, J. P. & Eberhart-Phillips, D. *J. geophys. Res.* **97,** 4843–4864 (1992).
40. Zhou, Y., McNally, K. C. & Lay, T. *Phys. Earth planet. Inter.* **75,** 267–288 (1993).
41. Jones, L. M., Hutton, L. K., Given, D. G. & Allen, C. R. *Bull. seism. Soc. Am.* **76,** 1830–1837 (1986).
42. Hauksson, E. & Jones, L. M. *Bull. seism. Soc. Am.* **78,** 1885–1906 (1988).
43. Hauksson, E. & Jones, L. M. *J. geophys. Res.* **94,** 9569–9589 (1989).
44. Magistrale, H., Jones, L. M. & Kanamori, H. *Bull. seism. Soc. Am.* **79,** 239–251 (1989).
45. Sipkin, S. A. *Bull. seism. Soc. Am.* **79,** 493–499 (1989).
46. Hauksson, E. *J. geophys. Res.* **95,** 15365–15394 (1990).
47. Wald, D. J., Helmberger, D. V. & Heaton, T. H. *Bull. seism. Soc. Am.* **81,** 1540–1572 (1991).
48. Beroza, G. C. *Bull. seism. Soc. Am.* **81,** 1603–1621 (1991).
49. Hauksson, E. & Jones, L. M. *J. geophys. Res.* **96,** 8143–8165 (1991).
50. Horton, S. P., dePolo, D. M. & Walter, W. R. *Bull. seism. Soc. Am.* (in the press).
51. Hauksson, E. *Bull. seism. Soc. Am.* **84,** 1058–1074 (1994).
52. Velasco, A. A., Ammon, C. J. & Lay, T. *J. geophys. Res.* **99,** 711–728 (1994).
53. Hauksson, E., Jones, L. M., Hutton, L. K. & Eberhart-Phillips, D. *J. geophys. Res.* **98,** 19835–19858 (1993).
54. Oppenheimer, D. *et al. Science* **261,** 433–438 (1993).
55. Hauksson, E., Jones, L. M. & Hutton, L. K. *J. geophys. Res.* **100,** 12335–12355 (1995).
56. Dixon, W. J. & Massey, F. J. *Introduction to Statistical Analysis* 119 (McGraw-Hill, New York, 1969).

ACKNOWLEDGEMENTS. We thank K. Smith, D. Oppenheimer, D. dePolo and M. Pasyanos for providing data and source parameters, and E. Smith for assistance with the statistical analysis. We also thank J. Vidale, D. Wald, P. Reasenburg, Y. Ogata and T. Webb for comments and suggestions which improved the manuscript. Catalogue data were obtained from the Northern California Earthquake Data Center, Southern California Earthquake Center Data Center, and University of Nevada, Reno. We are grateful to the USNSF, the USGS and SCEC for partial funding of this research.

A complete skeleton of the giant South American primate *Protopithecus*

Walter Carl Hartwig* & Castor Cartelle†

* Department of Anthropology, George Washington University, Washington DC, 20052, USA
† Instituto de Geociencias, Universidade Federal de Minas Gerais, Belo Horizonte, MG, Brazil

A COMPLETE skeleton of a large-bodied New World monkey has been found in Pleistocene cave deposits in the Brazilian state of Bahia. It demonstrates an unprecedented combination of body size, locomotor and cranial morphology. Skeletal features indicate an animal of approximately 25 kg, more than twice the mass of any living South American monkey. We refer the specimen to *Protopithecus brasiliensis* Lund, 1838, a large Pleistocene primate originally represented by only a proximal femur and distal humerus[1-4]. The skeleton resembles species of two distinct New World monkey lineages. The cranium is modified for an enlarged vocal sac typical of living howler monkeys[5-7], and the postcranium includes suspensory and brachiating components of locomotion as seen in living spider and woolly spider monkeys[8]. This skeleton confirms that adaptive diversity in neotropical primates was greater in the recent past, and that current interpretations of how their distinctive adaptations evolved should be revised.

The anatomy of the *Protopithecus* skeleton closely resembles the anatomy of the four largest living New World monkeys, typically of mass 6–12 kg and classified together at the subfamily rank (Atelinae). This New World monkey subfamily can be separated into a radiation of howler monkeys (tribe Alouattini, genus *Alouatta*) and atelin monkeys (tribe Atelini, genera *Ateles*, *Brachyteles*, *Lagothrix*)[5]. *Alouatta* is unique morphologically because of its unusually large hyo-laryngeal apparatus and the effects of this on the basicranium[6,7]. The atelin New World monkeys are characterized by relatively long forelimbs compared to hindlimbs, which reflects their adaptation to a suspensory positional repertoire and a brachiating mode of locomotion[8]. Howler monkeys locomote by a deliberate above-branch quadrupedalism[9,10], and thus their limb proportions are closer to equal. *Protopithecus* is remarkable because it displays cranial features typical of alouattins, but postcranial features characteristic of atelins.

Order Primates Linnaeus, 1758
Suborder Haplorhini Pocock, 1918
Infraorder Platyrrhini E. Geoffroy, 1812
Family Atelidae Gray, 1825
Subfamily Atelinae Gray, 1825

Protopithecus Lund, 1838

Protopithecus brasiliensis Lund, 1838, emended diagnosis.

Type specimen. Universitets Zoologisk Museum (UZM) 1623, a left proximal femur, and UZM 3530, a right distal humerus[4] of the same individual.
Hypodigm. The type, and Instituto de Geociencias, Universidade Federal de Minas Gerais (IGC-UFMG) 06, a nearly complete skeleton preserving cranium, mandible, several vertebrae, scapular and innominate fragments, upper and lower limb long bones, carpals, tarsals, metacarpals, metatarsals and phalanges.
Locality. The type specimen was recovered in 1836 in Lapa do Periperi, in the Pleistocene limestone cave network of Lagoa